Available online at www.sciencedirect.com
ScienceDirect
International Journal of Heat and Mass Transfer 50 (2007) 997–1009
International Journal of HEAT and MASS TRANSFER
www.elsevier.com/locate/ijhmt

Enhancement of pool boiling critical heat flux in dielectric liquids by microporous coatings

Mehmet Arik [a,*], Avram Bar-Cohen [b], Seung Mun You [c]

[a] GE Global Research Center, Thermal Systems Laboratory, Niskayuna, NY 12309, United States
[b] University of Maryland, Department of Mechanical Engineering, College Park, MD 20742, United States
[c] University of Texas at Arlington, Department of Mechanical and Aerospace Engineering, Box 19023, Arlington, TX 76019-0023, United States

Received 23 September 2005; received in revised form 2 August 2006
Available online 19 October 2006

Abstract

An experimental investigation into the effects of pressure and subcooling on the pool boiling critical heat flux from a bare silicon chip-like heater and from a silicon heater coated with microporous layers, is reported. The dual inline heater package was immersed in FC-72, a dielectric fluid, and the experiments were performed in the horizontal orientation, with subcooling varying between 0 K and 72 K, and the pressure between 101.3 kPa and 303.9 kPa. The maximum CHF values on the diamond-base microporous-coated silicon heater were found to reach 47 W/cm^2, at 3 atm and nearly 50 K of subcooling, and to provide an average enhancement of approximately 60% over the values attained with un-treated silicon surfaces. An available CHF correlation, with a reported standard deviation of 12.5% for un-treated surfaces over a large range of pressures, subcoolings, and surface conditions, was shown to predict the pressure and subcooling effects on CHF from the surface-enhanced chip with a standard deviation of 12%.

1. Introduction

Techniques for increasing passive pool boiling heat transfer with small-scale surface cavities, created by the application of porous coatings, mechanical machining of grooves, or growing of dendrites, have received considerable attention in recent years [1]. Many investigators believe that the microgeometries of these enhanced surfaces are able to increase vapor trapping and, hence, the active nucleation site density, leading to reduced surface superheat for boiling incipience and established nucleate boiling [2]. Others have argued that restructured – and particularly microporous – surfaces create capillary suction flows that support thin film evaporation and change the heat transfer mode to a complex two-phase flow with dry-out of thin internal films as the upper limit rather than the classical CHF. In the hope of shedding some additional light on the limiting heat transfer mechanism on such enhanced surfaces, the current study presents the results of an experimental investigation into the effects of pressure and subcooling on the pool boiling critical heat flux from a square, chip-like, silicon heater supported on a dual-in-line chip package and enhanced with a microporous coating.

1.1. Classical studies

Based on the pioneering work of Berenson in the 1960s [3], it has long been understood that, in addition to the salutary effect on the pool boiling critical heat flux, or "CHF", of pressure, subcooling, heater material, and thickness, surface modifications can be used to further raise the pool boiling limit. Berenson [3] extensively investigated the effect of surface finish on nucleate boiling performance, by studying the characteristics of pool boiling from surfaces with a high density of stable, artificially formed nucleation sites. Later, Costello and Frea [4] were among the first researchers to look at the surface effects with horizontally oriented stainless steel semi-cylindrical heaters in water. Coating the heaters with calcium carbonate was

* Corresponding author. Tel.: +1 518 387 5960.
E-mail address: arik@crd.ge.com (M. Arik).

0017-9310/$ - see front matter © 2006 Elsevier Ltd. All rights reserved.
doi:10.1016/j.ijheatmasstransfer.2006.08.005

Nomenclature

a	constant in Eq. (2)
b	constant in Eq. (2)
B	constant in Eq. (2)
c_p	specific heat, J/kg K
CHF	critical heat flux, W/m^2
DIP	dual inline package
g	gravitational acceleration, m^2/s
h_{fv}	latent heat of evaporation, J/kg
Ja	volumetric Jacob number, $(\rho_f c_p \Delta T_{sub})/(\rho_v h_{fv})$
L	heater length, m
P	absolute pressure, kPa
Pe	effective Peclet number, $[\sigma^{0.75}/(\alpha\rho_v^{0.5})g(\rho_f-\rho_v)^{0.25}]$
q''	heat flux, W/m^2
S	thermal activity parameter $[\delta\sqrt{\rho c_p k}]$
T	temperature, °C
α	thermal diffusivity, m^2/s
ρ	density, kg/m^3
ΔT	temperature difference, K
σ	surface tension, N/m

Subscripts

l	liquid
h	heater
sat	saturation
sub	subcooling
TME	thermal management of electronics
v	vapor

found to yield nearly 50% higher CHF values than on smooth heaters. They postulated that the increase in CHF for the treated surfaces was a result of increased wettability. Marto and Lepere [5] investigated the heat transfer enhancement of three commercially available surfaces (Union Carbide High Flux, Hitachi Thermoexcel-E, Wieland GEWA-T) on a cylindrical tube immersed in highly wetting liquids, such as saturated FC-72 and R-113. They observed a 60% decrease in nucleate boiling superheats and a negligible increase in CHF. Later, Chowdhury and Winterton [6] performed an experimental study to understand surface treatment and wettability effects. Experiments were conducted on copper and aluminum cylinders in methanol and water. They concluded that rougher heaters gave higher CHF values than polished surfaces. As early as 1974, a surface enhancement method to upgrade the nucleate boiling performance of silicon chips in dielectric liquids was devised by Oktay and Schmeckenbecher [7]. While it was shown possible to machine the surface of silicon chips to improve their heat transfer performance, such chip modifications were not usually permissible.

Mudawar and Anderson [8] found that the surface cavities, approximately 300 μm in diameter, were ineffective in lowering incipience superheats as well as enhancing CHF in FC-72. In a later publication [9], Mudawar presented an extensive summary of his team's studies on the surface enhancement of boiling, including the improvement associated with creating microstructures on the surface with sandpaper, silica blast surface finish, and microfin attachments. All of the surface attachments/treatments yielded some improvements in the FC-72 CHF values. The microstud-enhanced surface resulted in CHF values approaching 105.4 W/cm^2, while the CHF on microgroove enhanced surfaces reached as high as 92.8 W/cm^2 for this dielectric liquid.

Caravalho and Bergles [10] summarized the results of CHF enhancement by attached small heat sinks and treated surfaces, indicating that treated surfaces yielded higher CHF values than smooth surfaces, reaching values as high as 100 W/cm^2 for dielectric liquids at a bulk temperature of 25 °C, but that this effect could not be correlated by any single parameter or group of parameters.

1.2. Microporous coatings

In recent years great success in pool boiling enhancement has been achieved through the use of thin surface coatings [11]. It is generally thought that such enhancement results from a substantial increase in the nucleation site density and its uniformity across the heated surface. Alternatively, porous and microporous coatings can facilitate two-phase flow and boiling within the surface layer and produce substantial CHF augmentation.

Webb [12,13] found that the primary variables in microporous surface enhancement of pool boiling CHF were particle shape, coating thickness, and porosity and that particle size played a secondary role. Bergles and Chyu [14] observed an improvement in the boiling heat transfer with the use of commercial porous surfaces. Afgan et al. [15] studied the boiling characteristics from 30–75% porosity layers of sintered metal particles, using water, ethyl alcohol and R-113. They observed a qualitative change in the boiling mechanism at high heat fluxes and ascribed it to the presence of the sintered spherical particles. From these and related studies, it may be argued that much of this enhancement in CHF can be explained by the ability of the porous coating to smooth the transition from pool boiling to film boiling, facilitating the continuation of pool boiling on the outer surfaces of the porous layers, while vapor slugs – which may partially blanket the heated surface – form inside the coating.

Thome [16] reviewed a large number of data sets for pool boiling on porous coatings and found that, although these surfaces generally performed well, the optimum coating geometries in one study only vaguely corresponded to those found in others. The performance benefit of the coatings is thought to be due to the increase in the effective boiling

surface area, i.e., the vapor–liquid contact area, within the thick porous layer. Thome [16] also observed that three distinct evaporation mechanisms were present in porous coatings: thin film, capillary, and external evaporation, and that convective heat transfer could also be expected to prevail on the exterior surfaces, due to bubble agitation and vapor/liquid exchange, and inside the structure due to laminar flow through the "pores," possibly with strong entrance effects. In a later study, Chang and You [17] suggested that a lower porosity might lead to lower internal vaporization rates (thin film and capillary vaporization) due to reduced flow within the structure. While many of the enhanced surfaces tested have demonstrated the ability to reduce wall superheat and increase CHF, their feature sizes are apparently too large to effectively, trap a large number of embryonic bubbles when immersed in dielectric liquids [18].

You et al. [19] studied the enhancement potential of "particle layering," achieved by spraying particles on a flat surface and showed that a treated surface, immersed in saturated FC-72, could provide a 109% increase in CHF over the plain surface. O'Connor and You [20] reported a 224% larger CHF value when boiling with 45 K subcooling relative to the un-treated surface at saturated conditions in FC-72. Gulliksen et al. [21] also investigated enhanced boiling heat transfer with porous coatings for possible application to electronic cooling. A porous coating was made by gluing a 50 μm thick porous silver membrane on silicon heaters with thin layers of silver epoxy. A decrease in the incipience superheat and increase in the heat transfer rate were observed relative to plain surfaces, which were themselves superior to polished silicon surfaces. The authors concluded that the heat transfer coefficient scaled linearly with the permeability of the porous media and showed excellent agreement with this trend in their experimental results.

An experimental study of pool boiling of FC-72 in highly porous metal foam was reported by Arbelaez et al. [22], indicating that the temperature excursion usually observed for fluorinated fluids at the onset of nucleate boiling was not present and that an increase in the overall heat transfer performance and the CHF values, compared to flat, smooth plates was obtained.

The effect of microporous surfaces on nucleate boiling heat transfer in saturated FC-72 was studied by Kim et al. [23], using high-speed photography to study bubble size, bubble frequency, and vapor film characteristics on plain and coated thin wire heaters. The authors related the observed CHF enhancement to improved convective heat transfer as well as an increase in the velocity associated with the controlling hydrodynamic instability. Rainey et al. [24] studied CHF enhancement on flat copper heaters coated with microporous structures and immersed in FC-72, achieving a maximum CHF value of nearly 80 W/cm^2 and offering an empirical correlation based on their results and others from the literature. Later, combined results for enhanced microporous and pin finned structures on the heaters subjected to a range of pressures (between 30 and 150 kPa), subcoolings (as high as 50 K), and dissolved gas concentrations in FC-72 were presented [1], yielding a maximum CHF value of 61.4 W/cm^2. The relative enhancement of CHF on finned surfaces, from increased subcooling, was greater for microporous surfaces than for the plain finned surface, but it was found to fall below the values achieved with microporous coated heaters. In an extended review of microporous surface coating enhancement of pool and flow boiling, You et al. [1] reported a decrease in the boiling incipience with an increase in CHF and revealed that applied microporous coatings have been proven to survive up to 10 years of continuous service. They ascribed the CHF increase to higher bubble departure frequencies along with smaller bubble departure diameters, leading to a larger microconvection contribution and higher heat fluxes at a given wall superheat.

In more recent publications Honda et al. [25] reported on the effects of microfins and roughness on boiling from a silicon chip in FC-72. Both surfaces showed a considerable heat transfer enhancement, increasing CHF by a factor of 1.8–2.3, as compared to a smooth chip, roughly comparable to the surface area enhancement provided by the fins, with somewhat more significant enhancement for subcooled boiling than for saturated boiling. El-Genk and Parker [26] investigated the effects of subcooling on pool boiling of HFE-7100 from 3 mm thick porous graphite surfaces. Along with nucleate boiling heat fluxes more than five times higher and surface superheats significantly lower than those for a bare copper surface in the same experimental apparatus, CHF of the porous graphite surface was found to equal 31.8 W/cm^2 and 66.4 W/cm^2 for 0 and 30 K subcooled boiling, as opposed to CHF values for the smooth copper of 21.5 W/cm^2 and 37.3 W/cm^2, respectively, reflecting a greater enhancement for subcooled pool boiling than under saturated conditions.

Pool boiling on thin and uniform porous coatings was also examined experimentally [27] for various copper particle diameters and fabrications. The results show that the CHF is about 1.8 times higher for all the coatings. It was suggested that the presence of the thin, uniform porous coating influences the hydrodynamic instabilities responsible for CHF by statistically reducing the critical Rayleigh–Taylor wavelength and/or increasing the vapor area fraction. It was postulated that for a 2-fold increase in CHF, the unstable wavelength in the classical Kutateladze–Zuber CHF model would need to fall to nearly one-quarter of that for a plain surface. An experimental study was presented by Sebastine et al. [28] with carbon nano-tube coated silicon chips to understand the effect on boiling and CHF in FC-72. Test results revealed a CHF of approximately 15 W/cm^2 for a CNT-coated silicon wafer and a CHF of approximately 10 W/cm^2 for uncoated silicon.

2. Theoretical models

The earliest theoretical models for CHF are attributed to Kutateladze [29] and Zuber [30]. Noting the similarity between "flooding" in distillation columns and the CHF

condition, Kutateladze [29] obtained an expression for CHF based on a similitude analysis of the momentum and energy equations governing the two-phase flow near the heated surface. Subsequently, Zuber [30] derived an analytical equation for CHF by assuming that the Taylor hydrodynamic instability between up-flowing vapor columns and down-flowing liquid was the controlling mechanism. This analysis yielded the following relation for CHF:

$$q_{\mathrm{CHF}} = \frac{\pi}{24} h_{\mathrm{fv}} \sqrt{\rho_{\mathrm{v}}} [g\sigma_{\mathrm{f}}(\rho_{\mathrm{f}} - \rho_{\mathrm{v}})]^{1/4} \tag{1}$$

Eq. (1) was derived for a specific configuration, namely: saturated pool boiling of a liquid on an infinite, upward-facing horizontal plate. Despite these limitations, investigators have found it possible to use Eq. (1) in a wide variety of situations, and have introduced correction factors to account for the effects of specific parameters, such as subcooling and heater geometry.

While many correlations have been developed for predicting the pool boiling critical heat flux, only the thermal management of electronics (TME) correlation [31] includes the contribution of conduction in the heater together with the hydrodynamic, subcooling, pressure, and length effects. The TME correlation, written as a product of four terms, is given as follows [31]:

$$\begin{aligned} q''_{\mathrm{CHF,TME}} = {} & \frac{\pi}{24} h_{\mathrm{fv}} \sqrt{\rho_{\mathrm{v}}} [\sigma_{\mathrm{l}} g(\rho_{\mathrm{l}} - \rho_{\mathrm{v}})]^{1/4} \left(\frac{S}{S + 0.1} \right) \\ & \times [1 + \langle a - \mathrm{b} \times L'(P) \rangle] \\ & \times \left(1 + B \times \left[\left(\frac{\rho_{\mathrm{l}}}{\rho_{\mathrm{v}}} \right)^{0.75} \frac{c_{p_{\mathrm{f}}}}{h_{\mathrm{fv}}} \right] \Delta T_{\mathrm{sub}} \right) \end{aligned} \tag{2}$$

where $L'(P) = L\sqrt{\frac{g(\rho_{\mathrm{l}} - \rho_{\mathrm{v}})}{\sigma}}$ and $S = \delta_{\mathrm{h}} \sqrt{\rho_{\mathrm{h}} c_{\mathrm{h}} k_{\mathrm{h}}}$.

The first term on the right side of Eq. (2) represents the classical Kutateladze–Zuber prediction that is the upper limit, saturation value of CHF on very large horizontal heaters. The second term reflects the effect of heater thickness and thermal properties. The third term accounts for the influence of the length scale on the CHF and is equal to unity or higher. If the expression between the triangular brackets is a negative number, it must be set to zero. The last term represents the influence of subcooling on CHF. Following [32], the constants a and b in Eq. (2) have the values 0.3014 and 0.01507, respectively, for horizontal heaters immersed in dielectric coolants. Similarly, the constant B in Eq. (2) has the value 0.03 for horizontal heaters and 0.043 for vertical heaters immersed in dielectric coolants.

This composite correlation can be used to predict the CHF in a variety of situations by using the appropriate constants a, b and B. It includes explicitly the dependence of the CHF on the bulk thermal properties of the heater surface, such as thickness, thermal conductivity, and specific heat. This TME relation embodies the asymptotic dependence of CHF on the product of the heater thickness and the square root of thermal effusivity, reflecting the beneficial role of thermal conduction and absorption in smoothing the surface temperature resulting from non-uniform nucleation site density. It has been found that the TME correlation, Eq. (2), can predict the pool boiling critical heat flux with a standard deviation of 12.5% for various heater materials, geometries, and operating conditions, spanning the range of $0.2 < S < 120$, $0 < \Delta T_{\mathrm{s}} < 75$ K, and 100 kPa $< P <$ 450 kPa, and $4.7 < L' < 28$, within a 95% confidence level [31]. It has also been determined that beyond a value of 2, the thermal activity parameter, S, has no effect on CHF and that CHF is independent of L' for values larger than 20.

Regrettably, the TME correlation does not have the ability to analytically determine CHF on heaters coated with microporous layers. However, following Rainey et al. [24], it might prove possible to capture the enhancement afforded by such microporous coatings, relative to the saturated, large, thick horizontal heater, pool boiling predictions of Eq. (1), by a single empirical multiplier equal to approximately 1.8. Using this factor in Eq. (2), or alternatively, an empirical, saturated pool boiling, large horizontal heater baseline CHF value, it might be expected that the TME relation would then properly predict the sensitivity of the microporous CHF to heater size, heater thermal properties, and the fluid pressure and subcooling.

2.1. Heater property effect on CHF

Bernath [33] was, perhaps, the first researcher to investigate the effects of thermal properties and thickness of the heater on the CHF by observing that thicker heaters produced higher CHF than thinner structures. His research on vertically oriented cylindrical heaters in water was later extended to both solid and hollow cylinders. Experimental results revealed that the solid cylinders had about 43% higher CHF than hollow structures [33]. A study employing zirconium ribbon heaters immersed in toluene, was performed by Cole and Shulman [34]. Experimental results were similar to previously published studies, with 42% higher CHF for the thickest heater. Caravalho and Bergles [10] performed an extensive study on the thermal property effect. Their experimental study showed that thick copper blocks experienced higher CHF, but Eq. (1) was found to over predict CHF by as much as 50%.

Following closely on the proposals of Ramilson and Lienhard [35] and Unal et al. [36], the Watwe–Bar-Cohen TME model [37] is predicated on the assumption of an ever present non-uniform nucleation site density on the heater surface, which results in the formation of local vapor mushrooms, via lateral coalescence of individual vapor bubbles or the collapse of vapor columns. The depletion of the liquid under these vapor mushrooms then leads to the creation of local dry spots, whose temperature rises steeply under the influence of the imposed heat flux. This temperature rise rate is moderated by the ability of the underlying structure to locally absorb and/or conduct heat to parts of the heater still experiencing nucleate boiling.

If the temperature of the dry patch, at the end of the residence (or "hovering") time of the vapor mushroom,

exceeds the Leidenfrost temperature, the returning liquid is unable to quench the overheated surface, local dry-out proceeds to global dry-out, and CHF is said to occur. If the heater is very thin and has poor thermal properties, the dry patch temperature may exceed the Leidenfrost critical temperature soon after the formation of the first dry spots on the heater surface. CHF on such heaters will then be highly sensitive to the non-uniformities in the nucleation site density and dependent on the S value of the surface, yielding a diffusion-driven lower limit on CHF. At the other end of the spectrum, the heater thickness and effusivity values may be so large as to successfully absorb and conduct the heat away from the local dry patch for an extended period, thus keeping the dry patch temperature from exceeding the critical re-wet temperature. For such a high-S situation, the heater may be able to sustain the sequential formation and extinction of many dry spots, relying on the subsequent re-wetting of the surface to locally cool the surface back to the nucleate boiling regime. CHF on such heaters would, then, occur primarily due to a hydrodynamic instability resulting in an extensive interruption of liquid flow to the heater. The hydrodynamic instability models would, therefore, provide the upper or asymptotic limit for CHF. Both the diffusion limited and hydrodynamics limited asymptotes of CHF behavior, as well as the operating domain between these asymptotes, are captured in Eq. (2).

3. Motivation for present study

The preceding has revealed that microporous coatings can exert a strong influence over the CHF in the pool boiling of dielectric liquids. While the effects of the primary boiling parameters on the CHF encountered on bare surfaces in such fluids have been studied in detail (e.g. [8,18,32,38]), the effect of liquid pressure and subcooling on the pool boiling critical heat flux of surfaces with microporous coatings have not been systematically explored. Therefore, the present study aims to determine the beneficial effect of a microporous coating on the pool boiling CHF of dielectric liquids for a range of liquid pressures and subcoolings. A small silicon heater was used for these experiments. The chip thickness was selected in such a way as to provide an asymptotic thermal effusivity value of 4.7 and, thus, assure that thermal conduction in the heater would not affect the CHF. The results were compared with the predictions of Eq. (2).

4. Pool boiling CHF experimental study

4.1. Coated ATC chips

The current experiments were performed with the ATC2.6 chip packages, shown in Fig. 1a and b, obtained from Sandia National Laboratories [25]. These dual-in-line

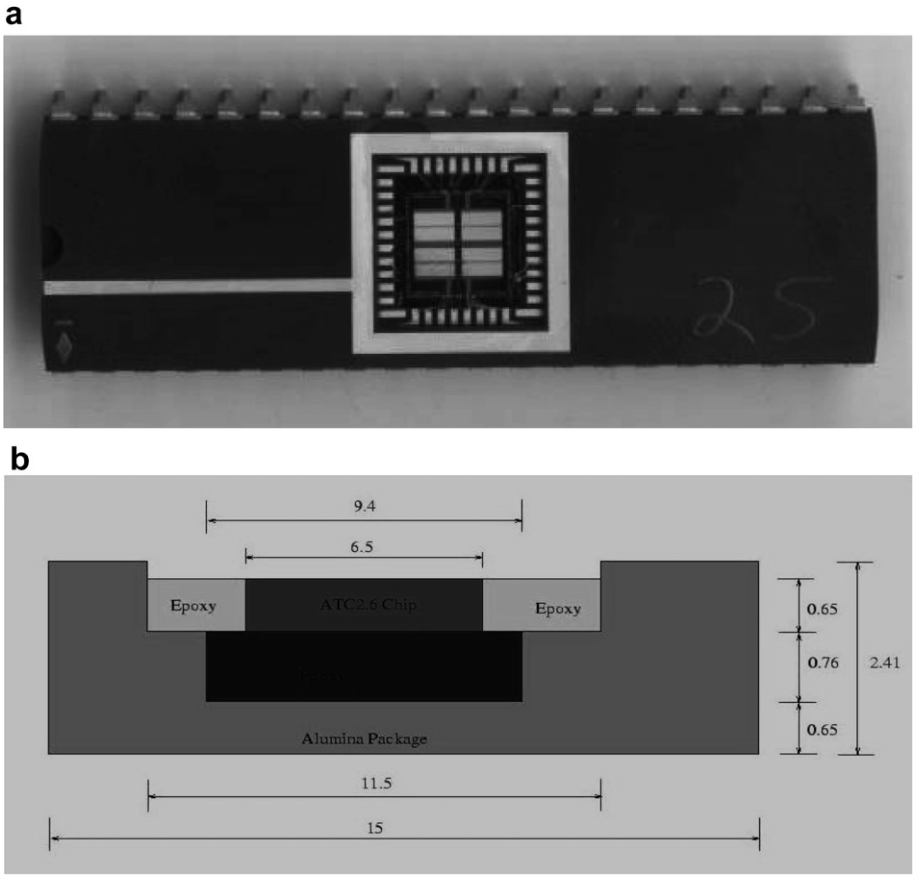

Fig. 1. (a) ATC2.6 Dual Inline Package, DIP by Sandia National Labs [25]. (b) Schematic diagram of the ATC2.6 chip packages [25].

chip packages (i.e., DIP) have 40 pins for providing power and ground connections and for extracting temperature signals from the embedded sensors. A silicon square die, 6.4 mm on each side, was embedded in a cavity and attached to the package by means of a low conductivity epoxy. The chip carries two heater structures on 2 μm lines and spacings, using poly-silicon conductors oriented perpendicularly to the overlying triple tracks with a nominal resistance of 50 Ω. This package provides five p^+n diode thermometers, one in the die center and four under the perimeter bond pads. Further details on the construction and assembly of the ATC2.6 package can be found in [38].

The thickness of the ATC2.6 chip was 625 μm before the coating was applied, yielding a value of the thermal activity parameter, S, for this silicon heater equal to 4.7. This S value should assure chip operation in the asymptotic hydrodynamic region where the bulk heater properties, including the contribution of the coating to the thickness and the effective effusivity, have no further effect on CHF. While the chip packaged within the 15 mm × 40 mm ATC2.6 package was just 6.5 mm on a side, the epoxy used to fill the surrounding cavity extended this characteristic dimension to 11.5 mm. Considering the possible influence of the package on the flow of liquid around the boiling chip, as well as the larger effective dimension of the chip itself, it can be assumed that this experiment did not benefit from the small heater, i.e., L', effect on CHF.

4.1.1. Coating

Several coating compositions of the type employed in the present experiments have been previously used for microscale enhancements [20]. The enhancement paint was manufactured by combining silver flakes with epoxy (Omegabond 101) and isopropyl alcohol. Later, diamond particles were used instead of silver flakes. A detailed examination of surface photographs of the diamond-omegabond-acetone (DOA), or diamond-brushable-ceramic (DBM) with MEK (i.e., methyl–ethyl–ketone), coating showed more uniform particle shapes and sizes of diamond [17], while the SOA coating displayed randomly oriented layers of silver flakes. The coatings are multi-layered microporous structures having thicknesses of approximately 100 μm for the CBM coating, 50 μm for the ABM and DOA (or DBM) coatings, and 30 μm for the SOA coating.

Chemical inertness was required for the binder for stable operation of these coatings. Since nearly identical boiling curves had been obtained for the three epoxies [17], Omegabond 101 epoxy was chosen for the current study. To create the microporous coating, 0.1 ml of Omegabond epoxy was used together with about 10 ml of Methyl Ethyl Ketone as the curing chemical for the coating applied to the ATC2.6 chips. Synthetic diamond powder with particle sizes of 8–12 μm was selected for the coating material. Approximately, 1.5 g of the powder was used to coat five ATC2.6 chip packages.

The following procedure was used to coat the chips. First, Omegabond 101 epoxy was placed into a glass vial and the vial was filled with Methyl Ethyl Ketone. The synthetic diamond powder was added into the vial. To obtain uniform mixture, the vial was carefully shaken. Next, an ultrasonic bath was used to achieve better mixing. A small amount of mixture was drawn into a pipet, and the mixture was dripped onto ATC2.6 chip surface. The coated chip was left in a well-maintained enclosure for overnight drying process. The drying process was performed under a regular light bulb to slightly elevate the temperature. The resulting coating thickness was approximately 50–75 μm. The resulting surface was termed a "microporous coated surface" since the coating thickness is less than 100 μm. Although, previous heater surfaces have been coated by using a paintbrush for small flat heaters and an airbrush for larger or irregular shaped heaters, due to their small size and protrusion from the package substrate, the ATC2.6 chips were coated exclusively by using this drip coating technique with a pipet [38].

4.2. Experimental apparatus

Fig. 2 shows the test set-up for the CHF experiments, originally designed by You [18] and modified for the current study. Experiments were conducted in a stainless steel test vessel operated at a pressure of up to 500 kPa. The tank includes two windows for the visual observation of the heat transfer phenomenon occurring on the chip surface. A lexan container filled with water is used to control the coolant temperature in the vessel. To condition the dielectric FC-72 test fluid, it is made to flow through a copper coil, which is immersed in the water. A magnetic stirring system is placed in the test vessel to create a uniform temperature distribution in the vessel.

A dual-type pressure gauge is connected to the flow loop to provide a visual display of the pressure and a piezo-resistive pressure transducer is installed on the cover of the test vessel. A precision resistor was used to accurately measure the current flowing in the power line. Temperature measurements were performed with diodes and thermocouples. The FC-72 temperature was measured by using five T-type thermocouples distributed in the liquid volume. The saturation temperature for FC-72 was reported to be 56 °C and 93 °C, at 1 atm and 3 atm, respectively [39]. Further details of this apparatus may be found in [38].

4.3. Experimental procedure

The data acquisition system consisted of a personal computer operating in the UNIX environment, a digital multi-meter with a 20-channel factory-built, scanner card. Power to the chip was supplied by a programmable DC power supply. A computer program, which worked in the UNIX environment, had been written to control the experiment and get the necessary readings from the system. The computer program controlled the power level, power incre-

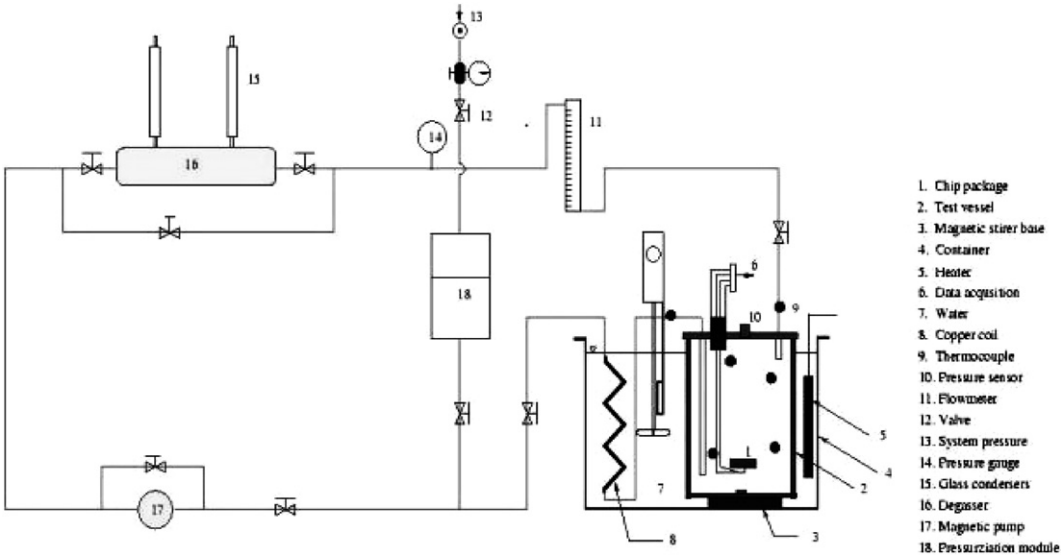

Fig. 2. Pool boiling experimental set-up [25].

ments, and readings. Approximately one hour before starting each test, all of the devices were turned on to avoid transient effects. The present experiments were performed with gas-saturated (i.e., gassy) coolant and no degassing procedure was followed. After the required test conditions were assured, the computer program was started. The computer program established the chip power setting and continuously read the diode temperatures to avoid a destructive termination of the experiment, i.e., "burn-out". At the end of the waiting period, when the steady state condition for each power level was attained, the final set of readings from diodes, thermocouples and pressure transducers was recorded in a file. Step sizes were varied between 0.2 and 1 W depending on the conditions. When a temperature jump of 30 K or more occurred, the computer program disabled the power supply. The experimental value of CHF was determined by averaging the last two heat fluxes, prior to the rapid rise in chip temperature.

4.4. Measurement uncertainty

Standard techniques were followed to obtain the experimental uncertainty [40]. The basic uncertainty sources were measurement resolution, substrate heat loses, and calibration errors. Precision errors from readings were decreased by increasing the sample population. The uncertainty in the wall superheat depends on both the surface and the saturation temperature. The overall uncertainty in the wall superheat was estimated to be ~1.5 K. The uncertainty in the actual heat flux from the chip was caused by variation in the voltage readings by the sensor and the current calculation through the precision resistor voltage readings. The maximum uncertainty in the heat flux was found to be 0.66 W/cm^2 within the 95% confidence level, at or near CHF. However, as a result of lower heat transfer coefficients from the package to the liquid during natural convection, the uncertainty in this part of the boiling curve, when heat fluxes are more moderate, is thought to equal ±1.8 W/cm^2. The dual-type pressure gauge in the FC-72 flow loop had a bias error of about 0.8%. The uncertainty associated with the pressure transducer installed on the cover of the test vessel is given by the manufacturer as 0.85 kPa.

5. Results and discussion

5.1. Boiling curves

Fig. 3a–c presents the boiling curves obtained with synthetic diamond coated ATC2.6 chip packages in FC-72. Boiling curves at three pressures are presented with various subcooling conditions. The pressure range was chosen between 101.3 kPa and 303.9 kPa, i.e., 1–3 atmospheres, while the bulk temperature varied between 21 °C and 55 °C for atmospheric pressure and between 21 °C and 74 °C for the 2 and 3 atm experiments.

Fig. 3a shows the boiling curves for the diamond-coated ATC2.6 chips, obtained from each of two runs at three subcooled liquid states in the FC-72 atmospheric pressure experiments The relatively high and repeatable CHF values, peaking at 38 W/cm^2 for the 21 °C liquid and 19.4 W/cm^2 for near-saturated FC-72, with a moderate shift in CHF superheat, provide direct evidence of the effectiveness of the microporous coating in enhancing pool boiling CHF. It may also be noted that a high degree of repeatability was achieved in the nucleate boiling part of the boiling curves, for each condition. On the other hand, the different subcoolings yielded somewhat different natural convection curves and moderate superheat variations even in the fully established nucleate boiling part of the boiling curve. Reflecting the strong statistical character of the incipience superheat overshoot observed in the pool

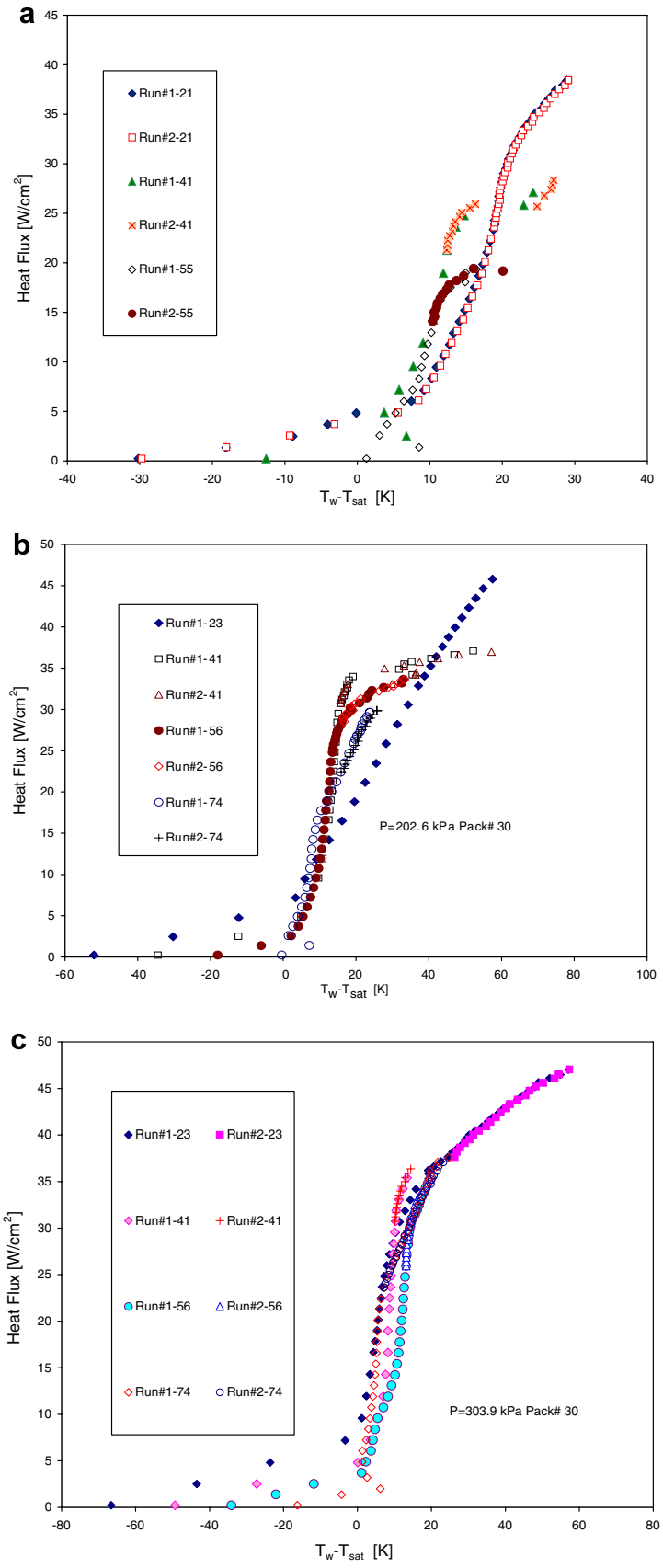

Fig. 3. (a) FC-72 boiling curves for coated ATC2.6 chip at atmospheric pressure and distinct liquid temperatures (21 °C, 41 °C, and 56 °C). (b) FC-72 boiling curves for coated ATC2.6 chip at two atmosphere pressure and distinct liquid temperatures (23 °C, 41 °C, 56 °C, and 74 °C). (c) FC-72 boiling curves for coated ATC2.6 chip at three atmosphere pressure with distinct liquid temperatures (23 °C, 41 °C, 56 °C, and 74 °C).

boiling of dielectric liquids [19,38], only one of the runs at near-saturated conditions (55 °C liquid) and one at 41 °C liquid clearly displayed this phenomena.

Small variations in fluid properties with liquid temperature, the non-linear dependence of natural convection on the surface-to-liquid temperature difference, and possible variations in dissolved gas concentration at the different dielectric liquid temperatures may explain these discrepancies. While pursuit of the boiling incipience behavior of the microporous coatings was beyond the scope of this study, it is instructive to note that Chang and You [17] observed a similar superheat overshoot at boiling incipience for saturated pool boiling on a microporous coated chip, while this phenomena was not observed in a more recent study [22].

The results attained with the diamond-coated ATC2.6 chip, displayed in Table 1, provide evidence of significant enhancement of the CHF relative to the uncoated ATC2.6 chip packages, with a maximum increase in CHF of 106% for the highly subcooled (35 K) liquid and 47% above the un-treated chip CHF when boiling at near-saturation conditions. It may also be noted that the slope of the boiling curves diminishes as CHF is approached. These results are in general agreement with previously reported surface enhancement studies showing more than 50% improvement in CHF with metal foams and coatings [17,22].

Fig. 3b presents the pool boiling results for the diamond-coated ATC2.6 chip operated at the seldom-reported pressure of 202.6 kPa, for liquid temperatures ranging from 23 °C to 74 °C. Each experiment was repeated at least two times, with additional runs performed for some of the operating conditions, and very good repeatability was observed. The highest CHF value was found to be 45.8 W/cm^2 at the lowest bulk temperature of 23 °C, yielding a 55% enhancement over the bare ATC2.6 chip. For the saturated liquid, at 74 °C, the CHF of 31 W/cm^2 was approximately 100% higher than the CHF on a bare chip.

Comparing these results with those shown in Fig. 3a, it may be seen that the 2-atm boiling curves shifted to the left, i.e., to lower superheats, especially in the nucleate boiling regime. However, as the curves approach the CHF limit, higher superheats were observed, especially for the highly subcooled liquid.

The pool boiling experiments with microporous coated ATC2.6 chips were completed by elevating the pressure to 3 atm (see Fig. 3c). A further shift of the boiling curves to the left, to lower superheats, was observed for the lower heat fluxes and moderate subcoolings. However, as noted for the 2 atm conditions, higher wall superheats were observed for the heat fluxes approaching the CHF limit, especially for the highly subcooled, 21 °C bulk temperature liquid, which reached a CHF value of 47 W/cm^2.

5.2. Critical heat flux on coated chips

As noted in the above discussion of the pool boiling curves, the microporous, diamond-coated ATC2.6 chips were found to provide CHF enhancement, relative to the bare chip, of from 36% to 103% for the three operating pressures and the range of subcoolings selected for these experiments. Table 1 provides an opportunity to examine these results in more detail. The experimental pressure and liquid temperatures are presented in the first and the second columns of the Table, while the corresponding liquid subcooling is given in the third column and column 4 provides the CHF values predicted by Eq. (2) for the experimental pressure and subcoolings shown. Columns five and six show the experimental findings, for the coated and bare chips, respectively, while column seven provides the observed CHF enhancement factor, displaying the ratio of the diamond coated CHF to the bare chip CHF. The next two columns provide the experimentally observed impact of pressure and subcooling on the CHF, expressed as the ratio of CHF at the stated conditions to the CHF at atmospheric pressure and near-saturation, i.e., 1.6 K of subcooling. It is to be noted that extrapolation of the experimental data to the atmospheric pressure, saturated liquid condition yields a bare chip CHF value of approximately 12.9 W/cm^2, some 2.5% lower than the near-saturated (1.6 K subcooling) value. Use of the extrapolated saturated value of CHF in Table 1 would, thus, have raised the indicated pressure and subcooling ratios by some 2.5%.

The tabulated experimental FC-72 CHF values for the bare chip, ranging from 13.2 W/cm^2 for near-saturated, 101 kPa liquid to 34.6 W/cm^2 for 304 kPa and 71 K of

Table 1
Pool boiling average experimental critical heat fluxes for microporous coated and uncoated silicon chips immersed in FC-72

P (kPa)	T (°C)	ΔT_{sub} (K)	CHF_{pred} (W/cm^2)	CHF_{coated} (W/cm^2)	CHF_{bare} (W/cm^2)	Coating enhancement	$\frac{CHF_{coated}}{CHF_{coated}\mid_{p=1\ atm,\ \Delta T=1.6\ K}}$	$\frac{CHF_{bare}}{CHF_{bare}\mid_{p=1\ atm,\ \Delta T=1.6\ K}}$
101.3	21	34.6	23.79	38.4	22.3	1.72	1.98	1.69
101.3	41	15.6	18.47	27.8	18.1	1.54	1.43	1.37
101.3	55	1.6	14.82	19.4	13.2	1.47	1	1
202.6	22	57	31.47	45.8	30.1	1.52	2.36	2.28
202.6	41	38	26.78	37.1	26.2	1.42	1.91	1.98
202.6	55	24	23.61	33.7	19.5	1.73	1.73	1.48
202.6	74	5	19.77	29.7	14.6	2.03	1.53	1.11
303.9	22	71.5	36.25	47.0	34.6	1.36	2.42	2.62
303.9	41	52.5	31.81	40.5	26.5	1.52	2.09	2.01
303.9	55	38.5	28.76	35.5	22.1	1.61	1.83	1.67
303.9	74	19.5	25.04	34.4	17.8	1.93	1.77	1.35

subcooling, are seen to be well predicted by the TME correlation, falling within the 12.5% standard deviation reported for this correlation [31]. The enhancement provided by the diamond microporous coating ranged from 36% to 103%, averaging approximately a 60% increase in CHF and providing values that ranged from 19.4 W/cm^2 at 1-atm and 1.6 K of subcooling to 47 W/cm^2 for 3-atm in 71 K of subcooling. Interestingly, these results suggest that the average diamond microporous coating enhancement factor of 1.6 was close to, though somewhat lower than, the 1.8 enhancement factor reported in [24]. The effect of pressure and subcooling on CHF, as reflected in the tabulated experimental CHF ratios, appears to be similar for the bare and coated chip, increasing with both pressure and subcooling relative to the respective near-saturated, 1 atm baseline. As previously noted, the increase in pressure from 2 atm to 3 atm appears to yield only a marginal improvement in the CHF, even in the presence of higher subcooling.

Fig. 4a shows the subcooling effect on the microporous diamond coated CHF for three distinct fluid pressures, presenting both the experimental findings and the linear equation obtained from a regression analysis. The relations between the CHF and subcooling, for each of the three operating pressures, and the resulting correlation factor are shown below:

$$\mathrm{CHF} = 0.5747 \times \Delta T + 18.61 \quad @\ 1\ \text{atm with}\ R^2 = 0.99 \tag{3a}$$

$$\mathrm{CHF} = 0.3051 \times \Delta T + 27.11 \quad @\ 2\ \text{atm with}\ R^2 = 0.95 \tag{3b}$$

$$\mathrm{CHF} = 0.2501 \times \Delta T + 27.97 \quad @\ 3\ \text{atm with}\ R^2 = 0.95 \tag{3c}$$

As anticipated, the CHF for the microporous coated chips is seen to increase nearly linearly with subcooling at all three pressures [41]. However, the effect of subcooling

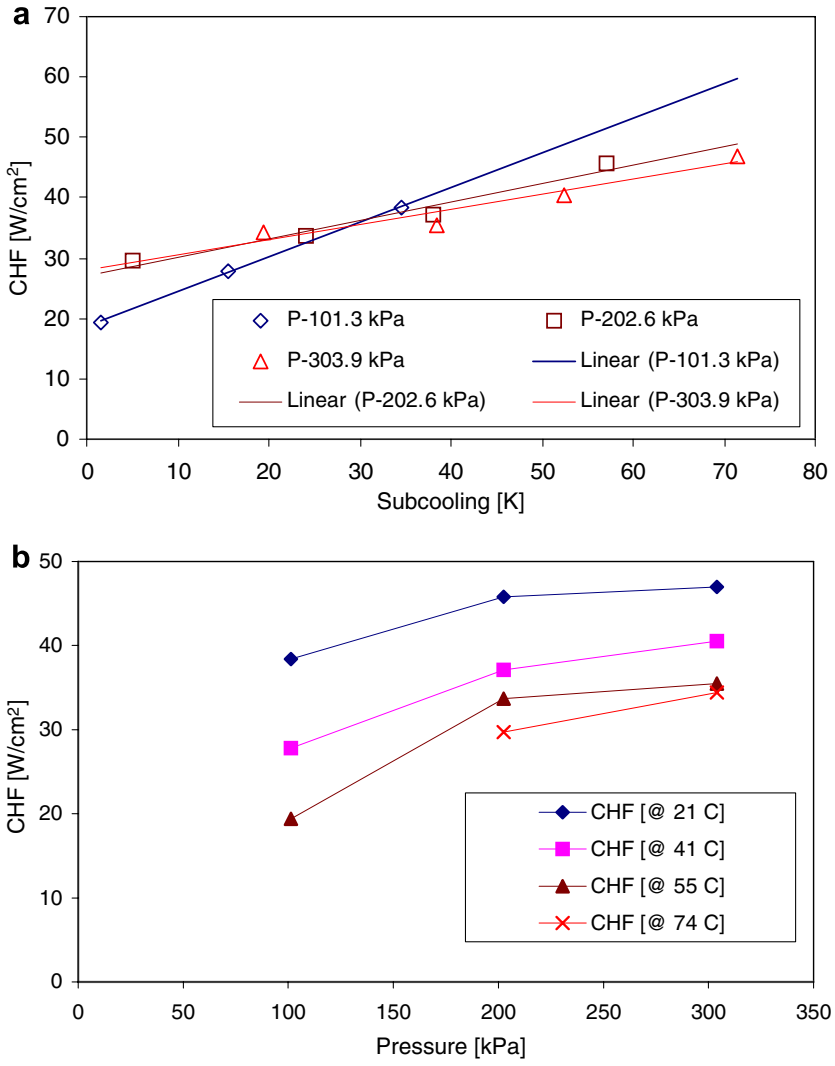

Fig. 4. (a) Effect of subcooling on constant pressure CHF for microporous diamond coated ATC2.6 chip immersed in FC-72. (b) Effect of pressure on subcooled CHF for microporous diamond coated ATC2.6 chip immersed in FC-72.

and the slope of Eq. (3), appear to diminish as the pressure increases, leading to a marginal increase in CHF as the pressure increases from 2 to 3 atm and the subcooling from approximately 60–70 K.

Pressure effects on the CHF values with coated ATC2.6 chip packages in FC-72 are shown in Fig. 4b at four different bulk temperatures. A strong increase in CHF can be observed as the pressure increases from 1 to 2 atm. However, as the pressure increases towards 3 atm, yielding the highest subcooling condition, the CHF values are found to be relatively insensitive to pressure and attain a peak value of 47 W/cm^2.

Fig. 5 presents the effect of the fluid pressure on the CHF from the current experimental study as well as published findings in [1,41]. It is found that both plain and coated chip surfaces experience a similar increase in pool boiling CHF.

Fig. 6 displays a comparison of the data obtained in this study with the TME-based prediction, Eq. (2), of the pressure and subcooling effects on pool boiling CHF. Both the bare chip and the diamond-coated chip data are shown normalized by the respective near-saturated, atmospheric pressure, pool boiling values obtained in this same study. It is instructive to note that all but one of the data points is seen to fall within a 15% error band, and the CHFs obtained with the microporous coated chips are thus within the variation previously determined for the TME correlation for un-treated surfaces over a large range of pressures,

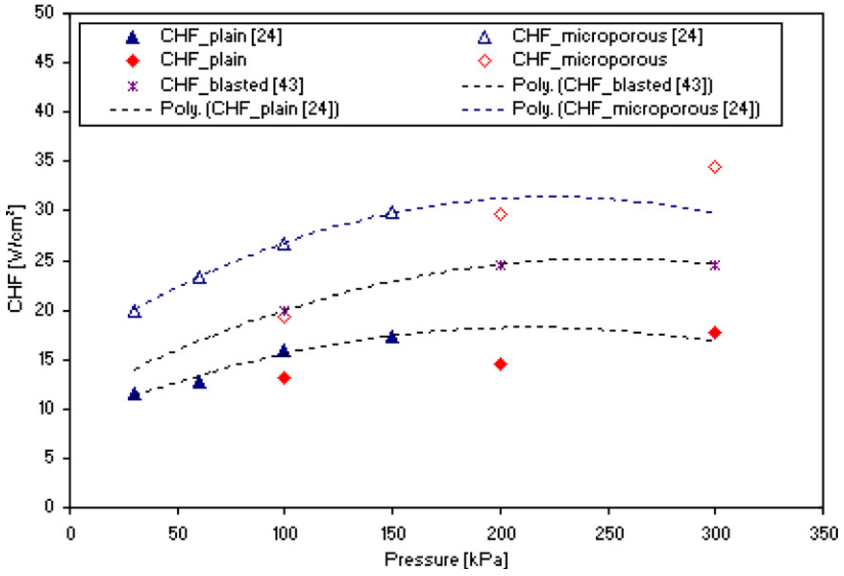

Fig. 5. Variation of CHF with the fluid pressure for various coated heaters.

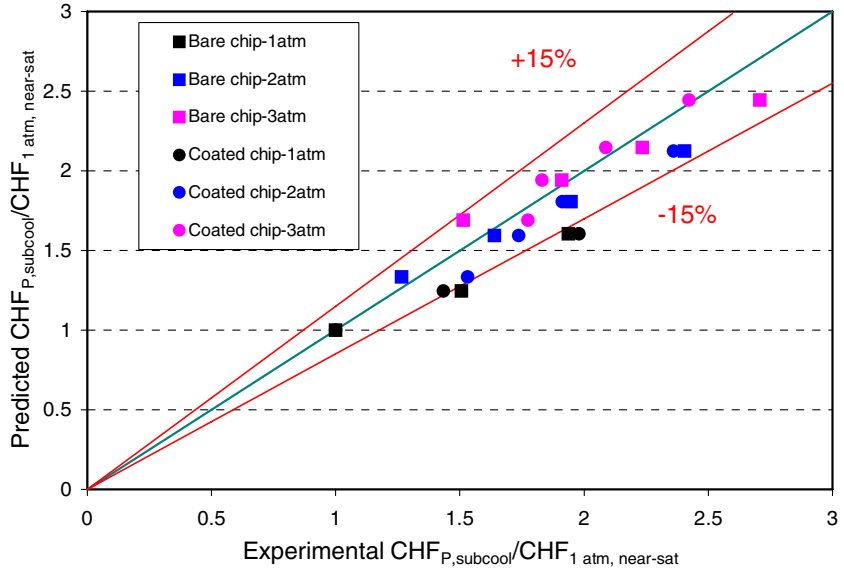

Fig. 6. Pressure and subcooling effect on CHF from microporous coated silicon chips.

subcoolings, and surface conditions. While additional parametric effects, such as the porosity, as well as the thermal properties and thickness of the coating, determine the extent of the CHF enhancement provided by surface coatings, the results displayed in Fig. 6 confirm that the effect of pressure and subcooling on the CHF of a specific microporous diamond coating is identical to that contained in the TME correlation. To capture the beneficial effect of the diamond microporous coating on pool boiling CHF, it should, thus, be sufficient to determine the CHF enhancement factor at just one pressure and subcooling and use the TME correlation to extrapolate this result to a wide range of pressures and subcoolings, as well as heater materials, thicknesses, and characteristic lengths.

For the specific diamond microporous coating used in this study, this porous coating enhancement factor was approximately 1.6. Additional experiments with a range of microporous coating morphologies and materials would be needed to determine the parametric sensitivity of this enhancement factor.

6. Summary and conclusions

The current experimental effort was devoted to understanding the pressure and subcooling effects of a microporous coating on the pool boiling critical heat flux, CHF, for square horizontal silicon heaters. Microporous, diamond-coated ATC2.6 chips were found to provide an average 1.6 enhancement factor on FC-72 CHF, relative to a bare chip, yielding values that ranged from 19.4 W/cm^2 at 1-atm and 1.6 K of subcooling to 47 W/cm^2 for 3-atm in 71 K of subcooling. The experimental FC-72 CHF values for the bare chip were well predicted by the TME correlation. The effect of pressure and subcooling on CHF appears to be similar for the bare and coated chips and to be well predicted by the pressure and subcooling corrections contained in the TME correlation, Eq. (2). To capture the beneficial effect of the diamond microporous coating on pool boiling CHF, it should, thus, be sufficient to measure the CHF at just one pressure and subcooling and use the TME correlation to extrapolate this result to a wide range of pressures and subcoolings, as well as heater materials, thicknesses, and characteristic lengths.

Acknowledgment

The authors are indebted to Mr. Dae Whan Kim for his invaluable help in processing the experimental data.

References

[1] K.N. Rainey, S.M. You, S. Lee, Effect of pressure, subcooling, and dissolved gas on pool boiling heat transfer from micro porous surfaces in FC-72, J. Heat Transfer 125 (2003) 75–83.
[2] S.M. You, K.N. Rainey, C.N. Ammerman, A new microporous surface coating for enhancement of pool ad flow boiling heat transfer, Adv. Heat Transfer 38 (2004) 73–141.
[3] P.J. Berenson, Experiments on pool boiling heat transfer, Int. J. Heat Mass Transfer 5 (1962) 985–999.
[4] C.P. Costello, W.J. Frea, A salient non-hydrodynamic effect on pool boiling burnout of small heaters, Chem. Eng. Prog. Ser. 61 (59) (1965) 271–280.
[5] P.J. Marto, Lt. V.J. Lepere, Pool boiling heat transfer from enhanced surfaces to dielectric fluids, Trans. ASME 104 (1982) 292–299.
[6] S.K.R. Chowdhury, R.H.S. Winterton, Surface effects in pool boiling, Int. J. Heat Mass Transfer 28 (1985) 1881–1889.
[7] S. Oktay, A.F. Schmeckenbecher, Preparation and performance of dendritic heat sinks, Solid-State Sci. Technol. 121 (1974) 912–918.
[8] I. Mudawar, T.M. Anderson, High flux electronic cooling by means of pool boiling – Part I: parametric investigation of the effects of coolant variation pressurization, subcooling and surface augmentation, in: 26th National Heat Transfer Conference, ASME HTD, vol. 111, ASME, New York, 1984, pp. 25–34.
[9] I. Mudawar, Direct-immersion cooling of high power electronic chips, in: Proc. ITHERM-III: Intersociety Conf. on Thermal Phenomena in Electronic Systems, 1992, pp. 74–84.
[10] R.D.M. Caravalho, A.E. Bergles, The effects of the heater thermal conductivity/capacitance on the pool boiling critical heat flux, in: Proc. Engineering Foundation Conf. on Pool and External Flow Boiling, Santa Barbara, 1992, pp. 203–212.
[11] R.L. Webb, Principles of Enhanced Heat Transfer, John Wiley, New York, 1992.
[12] R.L. Webb, The evaluation of enhanced surface geometries for nucleate boiling, Heat Transfer Eng. 2 (1981) 46–69.
[13] R.L. Webb, Nucleate boiling on porous coated surfaces, Heat Transfer Eng. 4 (1983) 71–82.
[14] A.E. Bergles, M.C. Chyu, Characteristics of nucleate pool boiling from porous metallic coatings, ASME J. Heat Transfer 104 (1982) 279–285.
[15] N.H. Afgan, L.A. Jovic, S.A. Kovalev, V.A. Lenykov, Boiling heat transfer from surfaces with porous layers, Int. J. Heat Mass Transfer 28 (1985) 415–422.
[16] J.R. Thome, Enhanced Boiling Heat Transfer, Hemisphere, New York, 1990.
[17] J.Y. Chang, S.M. You, Boiling heat transfer phenomena from microporous and porous surfaces in saturated FC-72, Int. J. Heat Mass Transfer 40 (18) (1997) 4449–4460.
[18] S.M. You, Pool boiling heat transfer with highly-wetting dielectric fluids, Ph.D. Thesis, Mechanical Engineering, University of Minnesota, Minneapolis, 1990.
[19] S.M. You, T.W. Simon, A. Bar-Cohen, A technique for enhancing boiling heat transfer with application to cooling of electronic equipment, IEEE Intersociety Conf. Thermal Phenom. Electron. Syst. (1992) 66–73.
[20] J.P. O'Connor, S.M. You, A painting technique to enhance pool boiling heat transfer in saturated FC-72, ASME J. Heat Transfer 117 (1995) 387–393.
[21] M. Gulliksen, H. Haugerud, H. Kristiansen, Enhanced boiling heat transfer with porous silver coatings for electronics cooling, in: Proc. ASME/JSME Thermal Engineering Conf., 1999.
[22] F. Arbalaez, S. Sett, R.L. Mahajan, An experimental study on pool boiling of saturated FC-72 in highly porous aluminum metal foams, in: 34th National Heat Transfer Conf., NHT2000-12192, 2000.
[23] J.H. Kim, K.N. Rainey, S.M. You, J.Y. Parl, Mechanism of Nucleate Boiling Heat Transfer Enhancement from Microporous surfaces in Saturated FC-72, Trans. ASME 124 (2002) 500–506.
[24] K.N. Rainey, S.M. You, Pool boiling heat transfer from plain and microporous, square pin finned surfaces in saturated FC-72, ASME J. Heat Transfer 122 (2000) 509–516.
[25] H. Honda, H. Takamastu, J.J. Wei, Enhanced boiling of FC-72 on silicon chips with micro-pin-fins and submicron-scale roughness, J. Heat Transfer ASME 124 (April) (2002) 383–390.
[26] M.S. El-Genk, J.L. Parker, Pool boiling in saturated and subcooled HFE-7100 dielectric fluid from a porous graphite surface, in: 2004 Inter Society Conference on Thermal Phenomena – ITHERM 2004, San Diego, CA.

[27] G.S. Hwang, M. Kaviany, Critical heat flux in thin, uniform particle coatings, Int. J. Heat Mass Transfer 49 (2005) 844–849.
[28] Sebastine O. Ujereh Jr., Issam Mudawar, Placidus B. Amama, Timothy S. Fisher, Weilin Qu, Enhanced pool boiling using carbon nanotube arrays on a Silicon surface, in: 2005 ASME International Mechanical Engineering Congress and Exposition, November 5–11, 2005, Orlando, FL, IMECE2005-80065.
[29] S.S. Kutateladze, A hydrodynamic theory of changes in the boiling process under free convection conditions, Izv. Akad. Nauk SSSR, otd. Tekhn. Nauk (No. 4, Translated in AEC-TR-1441), 1951, p. 529.
[30] N. Zuber, Atomic Energy Commission Report AECU-4439, Atomic Energy Commission Technical Information Service, 1959.
[31] M. Arik, A. Bar-Cohen, Effusivity-based correlation of surface property effects in pool boiling CHF of dielectric liquids, Int. J. Heat Mass Transfer 46 (2003) 3755–3765.
[32] A. Watwe, A. Bar-Cohen, A. McNeil, Combined pressure and subcooling effects on pool boiling from a PPGA chip package, J. Electron. Packag. (June) (1997) 95–105.
[33] L. Bernath, A theory of local-boiling burnout and its application to existing data, Chem. Eng. Prog. Symp. Ser. 56 (1960) 95.
[34] R. Cole, H.L. Shulman, Critical heat flux at sub-atmospheric pressures, Chem. Eng. Sci. 21 (1966) 723–724.
[35] J.M. Ramilson, J.H. Lienhard, Transition boiling heat transfer and film transition regime, J. Heat Transfer 109 (1987) 746–752.
[36] C. Unal, P. Sadasivan, R.A. Nelson, On the hot spot controlled critical heat flux mechanism in pool boiling of saturated fluids, Pool Ext. Flow Boil. – ASME (1992) 193–201.
[37] A.A. Watwe, A. Bar-Cohen, Modeling of conduction effects on pool boiling CHF of dielectric liquids, in: Proc. of National Heat Transfer Conf., 1997, p. 35.
[38] M. Arik, Enhancement of pool boiling critical heat flux in dielectric liquids, Ph.D. Dissertation, Department of Mechanical Engineering, University of Minnesota, MN, USA, 2001.
[39] 3M Specialty Fluids, 2000. Available from: <http://www.3m.com/market/industrial/fluids/library>.
[40] Robert J. Moffat, Describing the uncertainties in experimental results, Exp. Thermal Fluid Sci. (1988) 3–17.
[41] H.J. Ivey, D.J. Morris, Critical heat flux of saturation and sub cooled pool boiling in water at atmospheric pressure, in: Proc. 3rd Int. Heat Transfer Conf., vol. III, 1966, pp. 129–142.